In-situ high-pressure behaviors of double-perovskite Sr_2ZnTeO_6*

Han Dan-Dan(韩丹丹), Gao Wei(高 伟), Li Na-Na(李娜娜), Tang Rui-Lian(唐瑞莲), Li Hui(李 会), Ma Yan-Mei(马艳梅), Cui Qi-Liang(崔启良), Zhu Pin-Wen(朱品文)†, and Wang Xin(王 欣)‡

State Key Laboratory of Superhard Materials, Jilin University, Changchun 130012, *China*

(Received 19 September 2012; revised manuscript received 23 October 2012)

Structural and spectroscopic properties of Sr_2ZnTeO_6 (SZTO) were investigated by angle-dispersive synchrotron X-ray powder diffraction and Raman spectroscopy in a diamond anvil cell up to 31 GPa at room temperature. Although SZTO remained stable up to the highest pressure, the different pressure coefficients of the normalized axial compressibility were obtained as β_{ab}=8.16×10^{-3} GPa^{-1} and β_c=7.61×10^{-3} GPa^{-1}. The bulk modulus B_0 was determined to be 190(1) GPa by fitting the pressure–volume data using the Birch–Murnaghan equation of state. All the observed Raman modes exhibited a broadening effect under high pressure. The vibrational band υ_1 around 765 cm^{-1}, which is associated with the Te–O stretching mode in the basal plane of the TeO_6 octahedron had the largest pressure coefficient, and the Grüneisen parameters for all the observed phonon modes were also calculated and presented. These parameters could be used to measure the amount of uniaxial or biaxial strain, providing a fundamental tool for monitoring the magnitude of the shift of phonon frequencies with strains.

Keywords: crystal structure, high pressure, X-ray diffraction, optical spectroscopy

PACS: 91.60.Gf, 61.05.cp, 61.50.–f **DOI:** 10.1088/1674-1056/22/5/059101

1. Introduction

In the past few decades, the double-perovskite structured compounds with the general formula $A_2BB'O_6$ (A = alkaline, alkaline-earth, or rare-earth ions, B and B' = transition metal ions) have been studied extensively for their potential applications in ferroelectrics, catalysis, magnetic media, and microwave dielectrics.[1–5] Depending on their valences and relative radii, the B (B') sites can be occupied by two different transition metal ions, therefore a broad range of chemical and physical properties may be expected in this system. From the structural point of view, the ideal structure of $A_2BB'O_6$ double perovskites can be derived from the cubic perovskite ABO_3, and viewed as regular arrangements of corner-sharing BO_6 and $B'O_6$ octahedra that alternate along the three directions of the crystal lattice, while the voluminous A cations occupy the voids between the octahedra.[6–8] However, the combinations of lattice distortions and orderings of different types of B (B') cations lead to the reduction of symmetry from the ideal cubic structure, and even small changes in the tilting of the B (B')O_6 octahedra can lead to either a tetragonal or a monoclinic distortion in these compounds. These distortions, sometimes very subtle, are often the cause of the important physical, electronic, and magnetic properties of perovskites. Nevertheless, until recently the detailed crystallographic studies of these ordered double-perovskite oxides have not been reexamined systematically.

By varying temperature or pressure, it has been reported that a structural phase transition would occur in several ordered double perovskites. For example, Sr_2CoWO_6 is found to undergo a phase transition from tetragonal (space group $I4/m$) to monoclinic phase (space group $P2_1/n$) upon cooling, but it undergoes a phase transition from tetragonal to cubic phase (space group $Fm\bar{3}m$) upon heating;[9] Sr_2MgWO_6 crystallizes in a tetragonal structure ($I4/m$) at ambient conditions, and transforms to a cubic structure ($Fm\bar{3}m$) with increasing temperature;[10] Sr_2CaWO_6 and Ca_2MgWO_6 also have a sequence of phase transitions from monoclinic ($P2_1/n$) to tetragonal ($I4/m$) and then cubic ($Fm\bar{3}m$) with the increase of temperature;[11,12] Sr_2CoTeO_6, with room temperature monoclinic ($P2_1/n$) symmetry, transforms to tetragonal ($I2/m$) and then cubic ($Fm\bar{3}m$) structure with increasing temperature; and Sr_2MnTeO_6 has a complicated sequence of structural transitions ($P2_1/n \rightarrow I2/m \rightarrow I4/m \rightarrow Fm\bar{3}m$) with the increase of temperature.[13,14] These transformations, driven entirely by the changes in the interatomic distance, could also be easily brought about by subjecting the compounds to high pressures. Similarly, applying pressure is also shown to exert an important influence on these materials. For example, Sr_2CoWO_6 exhibites a transition from tetragonal to monoclinic phase at 2.2 GPa;[15] and Sr_2CaWO_6 appears to undergo a phase transition at 3.2 GPa as evidenced by its high-pressure Raman spectra.[16] Interestingly, changes in temperature or pressure may induce not only structural but also electronic changes.[17,18] Near the pressures of 2.1 GPa and 7.5 GPa,

*Project supported by the National Natural Science Foundation of China (Grant No. 51172091), the Program for New Century Excellent Talents in University, China, and the National Fund for Fostering Talents of Basic Science, China (Grant No. J1103202).

†Corresponding author. E-mail: zhupw@jlu.edu.cn

‡Corresponding author. E-mail: Xin_Wang@jlu.edu.cn

© 2013 Chinese Physical Society and IOP Publishing Ltd

electronic phase transitions were reported for Sr_2FeMoO_6 and Sr_2FeNbO_6, respectively.[19,20] While for the series of $Sr_2TbRu_{1-x}Ir_xO_6$, it has been found that $Sr_2TbRu_{0.3}Ir0.7O_6$ exhibits a valence state transition at low pressure.[21] Despite these structural or electronic transitions, some other double-perovskites were found to be structurally stable at high pressures: Sr_2MgWO_6, Ba_2MgWO_6, and $CaCuMn_6O_{12}$ were found to remain structurally stable up to 40 GPa, 34 GPa, and 31 GPa, respectively.[22–24]

From the above reports, it is interestingly found that the crystal structure of some double-perovskite materials, like Sr_2CoWO_6, Sr_2MnTeO_6, Sr_2FeMoO_6, all of which have the tetragonal structure (space group $I4/m$), can be considered to have the intermediate phase in the sequence of possible structural phase transitions from monoclinic to cubic symmetry. These structural characteristics lead to the investigation of structural stability in the tetragonal double-perovskite compounds by the effects of pressure or temperature. As an important microwave material, Sr_2ZnTeO_6 (SZTO) has not yet been investigated from the perspective of the structural behavior at high pressure. Besides, to our knowledge, only a few Raman studies on these double-perovskite oxides have been reported.[25,26] In this paper, we report the results of *in-situ* high-pressure X-ray powder diffraction and Raman spectroscopy experiments on the tetragonal double-perovskite Sr_2ZnTeO_6. It is found that the crystal structure of SZTO is very stable up to the highest pressure reached but different normalized axial compression coefficients are obtained.

2. Experiment

2.1. Sample preparation

The powder Sr_2ZnTeO_6 sample was prepared by a solid state reaction with raw materials $SrCO_3$ (99.995%), ZnO (99.995%), and TeO_2 (99.995%). The TeO_2 was added in 5 mol% excess due to its high volatility. First, stoichiometric amounts of the reacting compounds were mixed using ethanol as the medium in an agate mortar. Second, the mixed stoichiometric materials were pressed into pellets and then subjected to heat treatment. Finally, the pellets were heated to 1173 K, maintained for 12 h, then the temperature was increased to 1373 K and maintained there for another 12 h. The as-prepared samples were characterized under an inert atmosphere by laboratory X-ray diffraction using a 12 kW Rigaku D/max-γA system equipped with a proportional detector with Cu K_α (Ni-filter) radiation. A single phase was found and confirmed to be the tetragonal structure reported.[27]

2.2. Angle-dispersive synchrotron X-ray diffraction at high pressures

The X-ray diffraction at high pressure was obtained using synchrotron radiation at the beam line X17C of the National Synchrotron Light Source (NSLS), Brookhaven National Laboratory, and angle-dispersive X-ray diffraction (ADXRD) measurements were conducted from ambient pressure up to 30.9 GPa at room temperature. An on-line image plate recorded the angle-dispersive diffraction patterns as obtained using a monochromatic beam ($\lambda = 0.4066$ Å) focused down to 10 μm spot size. FIT2D software was employed to convert the image plate records into 2θ and intensities.[28] The sample was finely ground and pressurized using a diamond anvil cell (DAC) with 500 μm culet. A T301 stainless steel gasket was pre-indented to a depth of 80 μm with a 200 μm hole drilled in the center. The pressure-transmitting medium was a mixture of ethanol–methanol–water (16:3:1). The pressure was calibrated by using the well known ruby luminescence method.[29]

2.3. High-pressure Raman spectroscopy

The high-pressure Raman scattering measurements were performed at room temperature up to 31 GPa. One piece of the as-prepared samples was loaded into a gasketed DAC with a 4:1 methanol/ethanol mixture as the pressure-transmitting medium. Pressures were also measured with the ruby luminescence method. A commercial spectrometer (Renishaw in-Via Raman microscope) in combination with a charge-coupled device (CCD) detector was used to collect all the data in the back scattering geometry. The sample was excited at 514.5 nm by an argon-ion laser with a power of 10 mW.

3. Results and discussion

3.1. X-ray diffraction patterns at pressures

Recently, the crystal structure of SZTO was reexamined, and it was found to have $I4/m$ symmetry at room temperature, as evidenced by Raman analysis.[27] As shown in Fig. 1, the tetragonal structure of SZTO can be represented as a three-dimensional network of alternating ZnO_6 and TeO_6 octahedra, with Sr atoms occupying the interstitial space. In our sam-

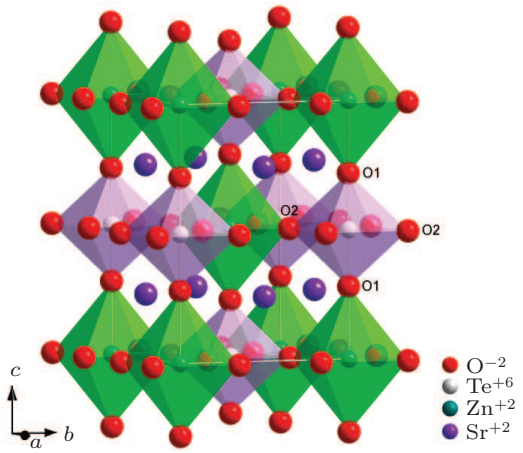


Fig. 1. (color online) Schematic representation of the crystal structure of Sr_2ZnTeO_6 (space group $I4/m$).

ple, the ambient-pressure diffraction pattern has been refined in the tetragonal phase (space group $I4/m$) with lattice constants $a = b = 5.6232(3)$ Å; $c = 8.0015(4)$ Å. In Fig. 2(a), the refined pattern is shown together with the calculated profile and their differences, and the merit of the refinement is $R_p = 5.6\%$, $R_{wp} = 7.8\%$, and $R_F^2 = 11.6\%$ at ambient pressure.

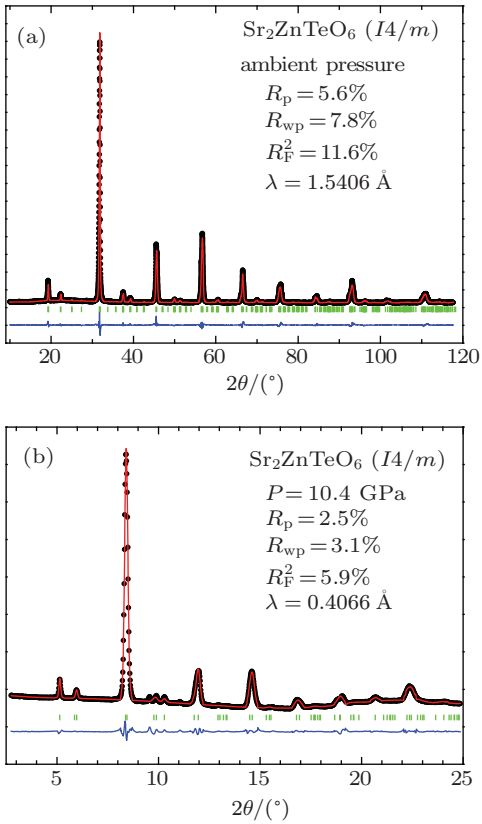


Fig. 2. (color online) Observed, calculated, and difference X-ray powder patterns of Sr_2ZnTeO_6 for the tetragonal phase: (a) Rietveld refinement at ambient pressure and (b) Le Bail fitting at 10.4 GPa.

Figure 3 shows a few representative X-ray diffraction patterns of SZTO at pressures up to 30.9 GPa. It can be seen that all the diffraction peaks shift toward higher 2θ values and exhibit some broadened features due to the evolved nonhydrostatic conditions with the increase of pressure. No obvious changes can be found in the diffraction patterns, suggesting that the crystal structure of SZTO is stable up to the highest pressure we reached. In order to determine the lattice parameters and the equation of state, Le Bail fitting of the tetragonal phase of SZTO was carried out at all the pressures by using GSAS software.[30] All the recorded diffraction patterns were analyzed with the help of Le Bail fitting, and the result was consistently excellent. Figure 2(b) shows the fitted pattern at 10.4 GPa with $R_p = 2.5\%$, $R_{wp} = 3.1\%$, and $R_F^2 = 5.9\%$. Besides, all changes in the relative unit-cell volume with pressure were fitted to the Birch–Murnaghan equation of state

$$p = \frac{3.0}{2} B_0 \left[\left(\frac{V_0}{V} \right)^{7/3} - \left(\frac{V_0}{V} \right)^{5/3} \right] \times \left\{ 1 + \frac{3.0}{4} \left(B_0' - 4 \right) \times \left[\left(\frac{V_0}{V} \right)^{2/3} \right] - 1 \right\}, \quad (1)$$

where B_0 and B_0' are respectively the bulk modulus and its pressure derivative at the equilibrium volume V_0. The pressure effects on the changes of unit-cell volume V are shown in Fig. 4(a). By fitting the equation, B_0 is calculated to be 190(1) GPa at fixed $B_0' = 4$, and the value is comparable to the bulk modulus of some other ordered double perovskites, for example, Sr_2MgWO_6, Ba_2MgWO_6, and $Sr_2TbRu_{0.3}Tr_{0.7}O_6$, which have the bulk moduli of 137 GPa, 128 GPa, and 196 GPa, respectively.[21–23] Furthermore, the compressions of the normalized unit-cell parameters are plotted in Fig. 4(b). As shown in Fig. 4(b), the compression behaviors differ along the crystallographic axes. It can be clearly seen that the c axis is less compressible than either the a or b axis, which indicates an increase in the magnitude of the octahedral tilting distortion. The different pressure coefficients of the normalized axial compressibility are obtained as $\beta_{ab} = 8.16\times10^{-3}$ GPa^{-1}, $\beta_c = 7.61\times10^{-3}$ GPa^{-1} with a linear fitting. The anisotropic compressibility could in principle bring about some significant changes in the electronic properties, as observed in Sr_2FeMoO_6 by Zhao *et al.*, so the electric measurement of SZTO at high pressure will be our future work.[19] This anisotropic compressibility might be explained by the typical structural features of these double-perovskite oxides. In general, the pressure has influences on the octahedral tilt angles and the associated B–O–B bond angles. As shown in Fig. 1(a), the structure of SZTO is made up of alternate corner shared octahedra, i.e., TeO_6 and ZnO_6. Along the c axis, these octahedra are connected through O1 atoms; and in the ab plane, they are connected by O2 atoms. Due to the special positions occupied by the Zn, O1, and Te atoms, along the c axis the bond angle of Zn–O1–Te is constrained to be 180°. In contrast, the calculated Zn–O2–Te bond angle in ambient conditions is 175.6°. Therefore, one might expect that the compressibility of Zn–O2 and Te–O2 bonds is larger than that of Zn–O1 and Te–O1 bonds, since more compression can be accommodated by further bending of the Zn–O2–Te angle. Similarly, as reported by Mishra *et al.*, the double-perovskite Sr_2MgWO_6 (SMWO) is structurally stable up to 40 GPa, and they predicted that the original tetragonal phase is more stable than the expected monoclinic structure up to at least 100 GPa according to first-principles calculations.[22] From their computed lengths of different cation–oxygen bonds (i.e., Mg–O1, Mg–O2, W–O1, W–O2), they speculated that the two bonds formed by oxygen atoms in the bending geometry in the ab plane were more compressible due to the weaker repulsion by the lone pair electrons of the oxygen atoms upon compression; in contrast, the two bonds in the linear geometry were less compressible because the presence of the lone pair of oxygen

atom electrons strengthened the repulsion upon compression. This is because both SZTO and SMWO have the same crystal structure and also a similar degree of lattice distortion at ambient pressure. Therefore the larger compression observed in the basal plane in SZTO, as compared to that along the c axis, could also be ascribed to the presence of the lone pair of electrons in the oxygen atom.

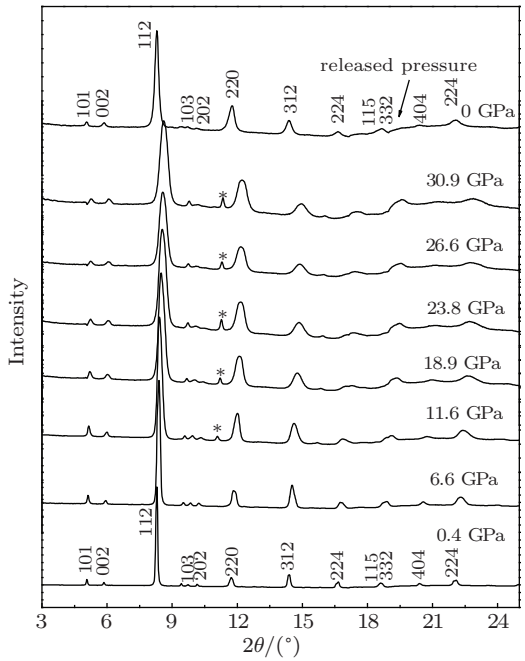


Fig. 3. Angle dispersive XRD patterns of Sr_2ZnTeO_6 at selected pressures with incident wavelength $\lambda = 0.4066$ Å at room temperature. The top pattern is decompressed from 30.9 GPa to ambient pressure. The asterisks mark the diffraction peaks from the gasket.

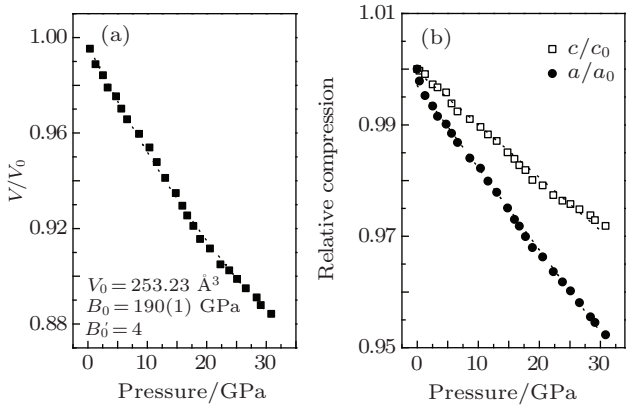


Fig. 4. (a) Experimental pressure–volume data of Sr_2ZnTeO_6 measured up to 31 GPa. The dotted line refers to the fitted Birch–Murnaghan equation of state. The corresponding parameters are given in the figure. (b) Variation of relative compression of the lattice parameters with pressure. Symbols represent the experimental data, and the dotted lines represented the linear fittings.

It has been reported that the structures of Ba_2MgWO_6 and Sr_2MgWO_6 remain stable up to 34 GPa and 100 GPa, respectively.[22,23] The stability of these two materials under compression is explained by considering the fact that in this type of compound only one of the octahedral site cations has the proper electron configuration to favor a second-order Jahn–Teller distortion. Since no displacement would be compensated by the non Jahn–Teller ions like Mg^{2+}, due to the needed appropriate bonding interaction with oxygen, a displacement would effectively destroy the cooperation of Jahn–Teller ions like W^{6+}. From this point of view, we might consider the same mechanism for SZTO, and this would be a plausible reason for the stability of SZTO under compression.

3.2. Pressure dependence of the vibration modes

The SZTO crystallizes in a tetragonal structure belonging to the $I4/m$ space group (No. 87, Glazer's notation $a^0a^0c^-$), this tetragonal structure could be derived from the prototype $Fm\bar{3}m$ cubic structure by an antiphase tilt of ZnO_6 and TeO_6 octahedra in the basal plane along the [001] direction of the cubic cell. In this structure, the Sr atoms occupy 4d sites with S_4 symmetry, the Zn and Te ions occupy 2a and 2b sites of C_{4h} symmetry, and the oxygen atoms are in the 8h and 4e sites (C_s and C_4 symmetries, respectively).

The Raman modes observed in the ambient spectrum in our experiment are consistent with those in the reported work.[27] According to Ref. [31], the distribution of the zone-center Raman active modes can be determined in terms of the irreducible representations of the C_{4h} point group using the method of factor group analysis

$$\begin{aligned}\Gamma_{\mathrm{R}}(I4/m) \;=\; & 2\mathrm{T}(\mathrm{B_g}+\mathrm{E_g})+2\mathrm{L}(\mathrm{A_g}+\mathrm{E_g}) \\ & +\upsilon_1(\mathrm{A_g})+\upsilon_2(\mathrm{A_g})+3\upsilon_5(2\mathrm{B_g}+\mathrm{E_g}).\end{aligned}$$

Here, υ_1 and υ_2 are related to the Te–O stretching modes, and υ_5 corresponds to the O–Te–O bending modes, T and L are translational and librational lattice modes, respectively. The highest frequency appearing in the Raman spectrum ($\upsilon >$ 700 cm^{-1}) is assigned to υ_1; those appearing in the range of 470–650 cm^{-1} are assigned to υ_2; those appearing in the range of 350–450 cm^{-1} are assigned to υ_5.

The Raman spectra of SZTO at various pressures up to 31 GPa were captured, and some selected Raman scattering spectra are shown in Fig. 5. With increasing pressure, all the Raman bands are shifted to higher frequencies, and there is no obvious change in the full Raman spectra. This result indicates that no structural transformation occurred in SZTO, which is consistent with the above X-ray diffraction result. As can be seen from Fig. 5, only five strong phonon modes are observed for SZTO in our high pressure experiments, and the modes located at 765 cm^{-1}, 568 cm^{-1}, 432 cm^{-1}, 422 cm^{-1}, 413 cm^{-1} are assigned to υ_1, υ_2, and $3\upsilon_5$, respectively. Due to strongly intercalating TeO_6 and weakly bonded ZnO_6 octahedra in the 1:1 order characteristics of SZTO, only the internal modes of the TeO_6 octahedron should be considered.[25] Thus, the observed Raman modes could be classified into O–Te–O bending vibrations in the 350–500 cm^{-1} region and Te–O stretching modes at frequencies over 500 cm^{-1}. These assigned fre-

quency regions have also been discussed in other similar double perovskites, such as Ba_2MWO_6 and Ba_2MMoO_6 (M = Ni, Co, Mg, Zn, Cd, Ca) and Pb_2MgWO_6.[25,32]

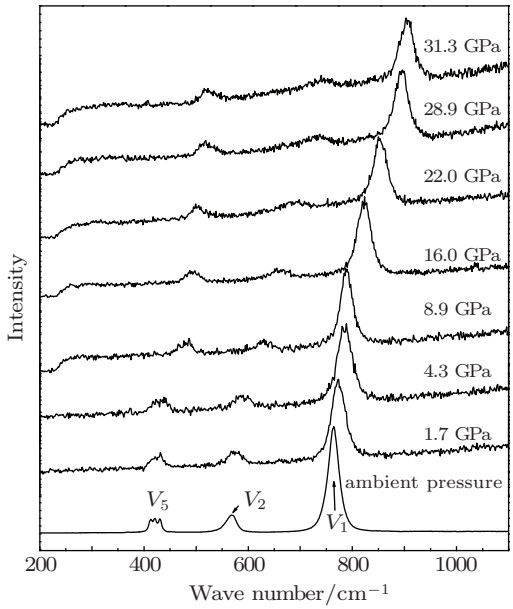


Fig. 5. Raman spectra of Sr_2ZnTeO_6 at different pressures. Spectra are recorded for a polycrystalline sample embedded in a methanol–ethanol mixture.

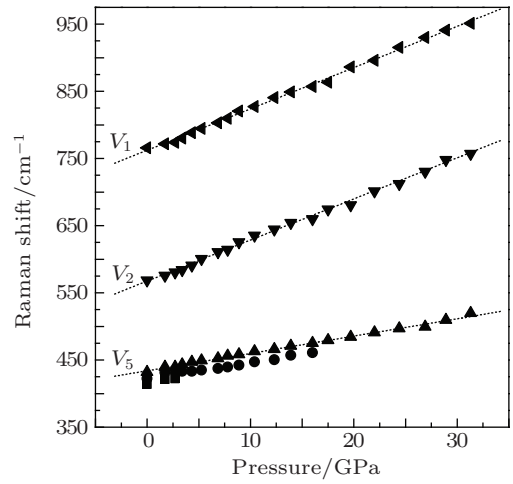


Fig. 6. Raman frequencies of Sr_2ZnTeO_6 as a function of pressure. The dotted lines represent the linear fittings.

As shown in Fig. 5, all the observed phonon modes (υ_1, υ_2, υ_5) exhibit gradually broadening effects with increasing pressure, and the pressure dependence of Raman phonon frequencies is shown in Fig. 6. All the observed phonon modes show a monotonous increase in frequency upon compression. The data for all the observed phonon modes could be fitted within experimental error by a linear relation $\Delta\omega(P) = AP$, where A is the first-order pressure coefficient. The values of the pressure coefficient for each mode are given in Table 1. We also list the calculated zero pressure mode Grüneisen parameter γ, defined as $\gamma = B_0 \frac{1}{\omega_i} \frac{d\omega}{dP}$, where ω_i is the initial frequency of the mode, and B_0 is the bulk modulus. The value of B_0 is 190(1) GPa taken from the high-pressure X-ray diffraction results above. Commonly, a strain arises when a crystal is compressed or stretched out of equilibrium, and the strain can modify the crystal phonons, with tensile strain usually resulting in mode softening and the opposite for compressive strain. The rates of these changes can be summarized in the Grüneisen parameter. The magnitude of the shift of phonon frequencies with strain is proportional to the Grüneisen parameter. As shown in Table 1, the value of the pressure coefficient of the υ_1 (765 cm^{-1}) mode that is assigned to Te–O stretching vibrations in the TeO_6 octahedra is the largest. This is consistent with the fact that the tilting and distortion of TeO_6 octahedra is pressure dependent, and these octahedra suffer much more strains in the *ab* plane than in their *c* direction. This is also evidenced by the different normalized axial compressibility of SZTO from the high pressure X-ray diffraction results.

Table 1. Observed phonon modes of Sr_2ZnTeO_6. The zero pressure frequency ω_0 and the linear pressure coefficient A are obtained by least-squares fits with a linear relation. The zero pressure mode Grüneisen parameter γ_0 is also presented.

	V_5	V_5	V_2	V_1
ω_0/cm^{-1}	422	432	568	765
A/cm^{-1}·GPa^{-1}	2.20(1)	2.58(1)	6.11(1)	6.14(2)
γ_0	0.99(1)	1.13(6)	2.04(2)	1.52(1)

4. Conclusion

In conclusion, the *in-situ* high-pressure behaviors of double-perovskite SZTO were investigated using angle-dispersive synchrotron X-ray powder diffraction and Raman spectroscopy in a diamond anvil cell at room temperature. The results indicated that the crystal structure is stable up to the pressures reached. From the results of high pressure X-ray diffraction, the different relative axial compression coefficients of SZTO were obtained as $\beta_{ab} = 8.16\times10^{-3}$ GPa^{-1}, $\beta_c = 7.61\times10^{-3}$ GPa^{-1}. The bulk modulus B_0 was determined to be 190(1) GPa by fitting the pressure–volume data using the Birch–Murnaghan equation of state. The high pressure Raman results were consistent with our X-ray diffraction data and indicated a stable crystal structure. The pressure dependencies of all the observed phonon modes were determined, and the strains from the TeO_6 octahedra were found to be responsible for the anisotropic compressibility of SZTO. Further investigations of other Te-based double-perovskite oxides under high pressure would be beneficial to understand the structural stability of these materials.

Acknowledgements

We acknowledge Dr. Chen Zhi-Qiang for technical support with the high-pressure experiments at the X17C beamline of the NSLS synchrotron.

References

[1] Kobayashi K I, Kimura T, Sawada H, Terakura K and Tokura Y 1998 *Nature* **395** 677

[2] DeMarco M, Blackstead, Dow J D, Wu M K, Chen D Y, Chien F Z, Haka M, Toorongian S and Fridmann J 2000 *Phys. Rev. B* **62** 14301

[3] Xiao C J, Chi Z H and Li F Y 2007 *Chin. Phys.* **16** 3125

[4] Burzoa E, Balasz I, Valeanu M and Pop I G 2011 *J. Alloys Compd.* **509** 105

[5] Geng H Y, Wu Q and Tan H 2002 *Chin. Phys.* **11** 1188

[6] Woodward P M 1997 *Acta Crystallogr. B* **53** 32

[7] Deng L W, Zhao J J, Ji G F, Gong Z Z and Wei D Q 2006 *Chin. Phys. Lett.* **23** 2334

[8] Howard C J, Kennedy B and Woodward P M 2003 *Acta Crystallogr. B* **59** 463

[9] Hahn T 2002 *International Tables for Crystallography* Vol. A

[10] Achary S N, Chakraborty K R, Patwe S J, Shinde A B, Krishna P S R and Tyagi A K 2006 *Mater. Res. Bull.* **41** 674

[11] Gateshki M and Igartua J M 2004 *J. Phys.: Condens. Matter* **16** 6639

[12] Yang J H, Choo W K and Lee C H 2003 *Acta Crystallogr. C* **59** i86

[13] Ortega-San Martin L, Chapman J P, Lezama L, Sanchez-Marcos J, Rodriguez-Fernandez J, Arriortua M I and Rojo T 2005 *J. Mater. Chem.* **15** 183

[14] Ortega-San Martin L, Chapman J P, Hernandez-Bocanegra E, Insausti M, ArriortuaM I and Rojo T, 2004 *J. Phys.: Condens. Matter* **16** 3879

[15] Manoun B, Igartua J M, Gateshki M and Saxena S K 2008 *J. Mol. Struct.* **888** 244

[16] Manoun B, Igartua J M, Gateshki M andSaxena S K 2004 *J. Phys.: Condens. Matter* **16** 8367

[17] Li M, Gao C X, Ma Y Z, He C Y, Hao A M and Zhang D M 2007 *Chin. Phys. Lett.* **24** 1010

[18] Zhang H, Tang J and Cheng X L 2008 *Chin. Phys. Lett.* **25** 552

[19] Zhao P, Yu R C, Li F Y, Liu Z X and Jin M Z 2002 *J. Appl. Phys.* **92** 1942

[20] Zhao X, Yu R C, Yao L D, Li F Y, Liu Z X, Bao Z X, Li X D, Li Y C, Ma M N, Liu J, Tang G D and Jin C Q 2004 *J. Phys.: Condens. Matter* **16** 1299

[21] Zhou Q, Kennedy B J, Wallwork K S, Elcombe M M, Lee Y and Vogt T 2005 *J. Solid State Chem.* **178** 2282

[22] Mishr A K, Poswal H K, Acharya S N, Tyagi A K and Sharma S M 2010 *Phys. Status Solidi B* **247** 1773

[23] Meenakshi S, VijayakumarV, Achary S N and Tyagi A K 2011 *J. Phys. Chem. Solids* **72** 609

[24] Zhang W, Yao L D, You S J, Yang L X, Yang H and Li F Y 2007 *Chin. Phys. Lett.* **24** 536

[25] Liegeois-Duyckaerts M and Tarte P 1974 *Spectrochim. Acta B* **30** 1771

[26] Baldinozzi G, Sciau Ph and Bulou A 1995 *J. Phys.: Condens. Matter* **7** 8109

[27] Dias A, Subodh G, Sebastian M T and Moreira R L 2010 *J. Raman Spectrosc.* **41** 702

[28] Hamersley P, Svensson S O, Hanfland M, Fitch A N and Dauserman D 1996 *High Pressure Res.* **14** 235

[29] Mao H K and Bell P M 1978 *Carnegie Institution of Washington Year Book* **77** 904

[30] Larson A C and Von Dreele R B 2004 *General Structure Analysis System (GSAS) Los Alamos National Laboratory Report LAUR* **86** 748

[31] Ayala A P, Guedes I, Silva E N, Augsburger M S, Viola M C and Pedregosa J C 2007 *J. Appl. Phys.* **101** 123511

[32] Baldinozzi G, Sciau P and Bulou A 1995 *J. Phys.: Condens. Matter* **7** 8109